14

The Hanbury-Brown-Twiss effect and the polarisation effects in the Lund model

14.1 Introduction

In this chapter we consider two different observables, which, within the Lund model, have some bearing upon the confinement properties of QCD.

We start with the Hanbury-Brown-Twiss effect (the HBT effect) or, as it is also called, the Bose-Einstein effect. It originated in astronomical investigations, [78], where one uses the interference pattern of the photons to learn about the size of the photon emission region, i.e. the size of the particular star which is emitting the light.

The Goldhabers, [65], found and used in the same way as HBT a correlation pattern among the produced pions when they investigated proton-antiproton annihilation reactions close to the threshold (i.e. when the annihilation occurs at very low relative velocities, so that the total energy is essentially twice the proton rest mass). Photons and pions have in common that they are bosons, which means that they thrive on being in the same state. The HBT effect can be described as an enhancement of the two-particle correlation function that occurs when the two particles are identical bosons and have very similar values of their energy-momentum.

The size of the emission region obtained from these experiments in hadronic physics seems to be essentially the same in almost any kind of interaction. One obtains a radius of the order of 1 fm, which is a very reasonable size. The extraction of this size as well as the finer details are, however, still under intense discussion, [93], because it is very difficult to determine the relative energy-momentum of the high-energy particles to the necessary precision. We first discuss the idea behind the chaotic interference pattern which is at the basis of the HBT effect. After that we consider the reason why the source size should be similar for the above-mentioned annihilation reaction at rest (which then is a 'low-energy

https://doi.org/10.1017/9781009401296.014 Published online by Cambridge University Press

reaction') and in a truly high-energy hadronic reaction when the decay products move apart with large velocities.

According to the way we have described the final-state particle production in the Lund model the particles emerge over a large (longitudinal) space-time region, which increases with the energy. Nevertheless it turns out that *it is only the local proper times for the production vertices which play a role in the correlation measurement*. All the proper times are essentially the same for the production vertices in the Lund model and it is this value that will determine the HBT effect. It may very well be the same size in the Goldhaber annihilation measurements also.

We will discuss the implications of the Lund string model for the phenomenon. We will in particular show that the matrix element $\mathcal{M}$, which we derived in Chapter 11, provides a precise prediction, [22], for the HBT effect in an e^+e^- annihilation event. This prediction is in good agreement with the data but there is nevertheless one problem left. In the string model for the HBT effect presented in [22] it is necessary to neglect the fact that a large amount of the pions are decay products of resonances. From ordinary quantum mechanical considerations one expects that the wave functions of the produced pions are affected if the pion stems from such a decay. It is not possible to explain the observed HBT effect if one removes the pions which stem from long-lived resonances or modify their wave functions in accordance with the expectations from the resonance wave functions. It was, however, pointed out by Bowler, [34], that the main problem relates to the Lund model rate for η'-mesons. If that rate is decreased then the predicted HBT effect from [22] is restored to almost the same size even if decay pions are included, i.e. it is essentially in agreement with experiment.

The HBT effect is, as mentioned, also seen in other reactions beside e^+e^- annihilation events. For the case of DIS, deep inelastic scattering, there is also a single string in the Lund model scenario; cf. Chapter 20. Therefore all the considerations in our discussion of e^+e^- annihilation reactions are also relevant to this case. However, for hadro-production and for large gluon activities in general it is not evident how to treat the HBT effect within a model of the Lund type. We will not, therefore, in this book comment upon this topic for hadronic reactions, due to the lack of a sufficiently structured model with which to investigate the effect in these reactions.

The second subject in this chapter is the polarisation properties which are observed in high-energy processes. The momentum distributions of the final-state hadrons are to a large extent governed by longitudinal phase-space size and therefore polarisation properties offer a tool for gaining insight into the 'other dimensions' of the hadronisation process.

Actually, polarisation effects have always been expected to die away at large energies because it has been hoped that for 'asymptopia' there

https://doi.org/10.1017/9781009401296.014 Published online by Cambridge University Press

would be only a single production amplitude, which would dominate the processes. Under such circumstances there would be no polarisation because, according to conventional models, such a phenomenon necessitates interfering production amplitudes.

Nevertheless, even at the largest energies available there are strong polarisation effects noticeable in inclusive Λ-particle production. This cannot be explained from hard scattering processes as calculated in QCD and therefore it should stem from the soft confining interactions. We also note that the observed polarisation is not a large-angle phenomenon. It seems to saturate already at transverse momenta of the order of 1 GeV/c.

It is interesting to note that polarisation will come out naturally in a confined production scenario like the Lund model. An intuitive argument is that in a confined field there is always a local direction, the force direction **n**, i.e. the direction of the flux of the color electric field. This means that, if we have a final-state particle which moves outwards with a momentum **p** not parallel to the direction **n**, there is a nonvanishing axial vector, **a**, obtained from the vector product $\mathbf{a} = \mathbf{n} \times \mathbf{p}$. A general experience of physics in any context is that wherever a possibility exists, Nature makes use of it. In this case it means that there is the possibility of a scalar coupling, in the overall hamiltonian, between the spin vector **S** of the quantum and the axial vector **a**. (Note that all angular momentum vectors have an axial character.)

We will provide a simple semi-classical model, [9], in which this is a very noticeable effect. We will show the difference between a confined scenario and the production of e^+e^--pairs in an external electromagnetic field. We have used this picture before to illustrate various features. Polarisation properties are one of the few cases where there are major differences between the the dynamics of QED and of QCD. The other cases considered in this book are the behaviour of the running coupling constant, Chapter 4, and the growth of the phase space in multigluon emissions, Chapter 17.

We will be content to apply the model to the polarisation properties of the Λ-particle in baryon fragmentation. It is possible to provide many more predictions using the model but that would mean that we would need a more elaborate formalism.

14.2 The Hanbury-Brown-Twiss effect

1 The classical argument, coherence and chaos

The arguments in this subsection are based upon the discussion in [33]. We will consider the production of pions from a set of sources localised at different positions $\mathbf{x}_j$. Each of them will have some time-dependent

https://doi.org/10.1017/9781009401296.014 Published online by Cambridge University Press

wave function $f_j(t_j)$. Then the total amplitude for emission of a pion with energy-momentum $(\omega_1, \mathbf{k}_1)$ is given by

$$A_1 = \sum_j f_j(t_j) \exp[i(\mathbf{k}_1 \cdot \mathbf{x}_j - \omega_1 t_j)] \tag{14.1}$$

The joint amplitude for emission of pions with energy-momentum vectors $(\omega_\ell, \mathbf{k}_\ell)$, $\ell = 1, 2$, is then evidently given by the double sum

$$A_{12} = \sum_j f_j(t_j) \exp(-ik_1 x_j) \sum_\ell f_\ell(t_\ell) \exp(-ik_2 x_\ell) \tag{14.2}$$

where we have used four-vector notation in the complex exponentials. We note that this corresponds to a totally symmetric amplitude. This is necessary because the pions are bosons.

According to quantum mechanics the emission probability is proportional to the square of the amplitude, $P_{12} \propto |A|_{12}^2$, i.e.

$$P_{12} \propto \sum_{i,j,k,\ell} \exp(-ik_1 x_j) \exp(-ik_2 x_\ell) \exp(ik_1 x_i) \exp(ik_2 x_k) \times f_j(t_j) f_l(t_\ell) f_i^*(t_i) f_k^*(t_k) \tag{14.3}$$

The basic idea in the HBT effect is to assume that the wave functions of the sources are wildly fluctuating so that there are only contributions to the sums above if

$$j = i, \ell = k \quad \text{or} \quad j = k, \ \ell = i \tag{14.4}$$

This is called the *chaotic limit* and we then obtain, writing $\rho_j = |f_j|^2$ for the source densities and exchanging the sums for integrals,

$$P_{12} \to \int dx_j dx_\ell \rho_j \rho_\ell [1 + \exp(iq\Delta x)] \tag{14.5}$$

We have here introduced the notation

$$q = k_1 - k_2, \quad \Delta x = -x_j + x_\ell \tag{14.6}$$

The result is evidently that

$$P_{12} = R^2(0) \left(1 + \frac{|R(q)|^2}{R^2(0)} \right) \tag{14.7}$$

in terms of the Fourier transform of the sources

$$R(q) = \int dx \exp(iqx) \rho(x) \tag{14.8}$$

If we calculate the one-particle yield in the same chaotic limit we obtain

$$P_1 = \sum_{ij} \exp(-ik_1 x_j) \exp(ik_1 x_i) f_j(t_j) f_i^*(t_i) \to \int dx \rho(x) = R(0) \tag{14.9}$$

https://doi.org/10.1017/9781009401296.014 Published online by Cambridge University Press

and we note that $R(0)$ is a real, positive number. We conclude that the normalised two-particle correlation function in this case will be

$$C_{12}^{HBT} = \frac{P_{12}}{P_1 P_2} = 1 + |\mathscr{R}(q)|^2 \tag{14.10}$$

where $\mathscr{R}$ is the normalised Fourier transform of the source densities,

$$\mathscr{R}(q) = \frac{\int \rho(x) dx \exp(iqx)}{\int \rho(x) dx} \tag{14.11}$$

In this way we measure by means of the two-particle correlations something very similar to a *form factor of the source*. We conclude, just as we did for form factors, that the Fourier transform is sensitive to $(-q^2)$-values larger than the inverse squared length scale of the source. In principle it should even be possible to deduce the detailed shape of the source by performing the inverse Fourier transform. However, there is not only the problem that we lack a knowledge of the phases; it is also a sad fact that it is difficult to obtain sufficiently precise experimental data to distinguish between even very different assumptions on the general shape of the source.

The only thing upon which all experiments seem to agree is that there is one size-scale, of order 1 fm. There is no noticeable change in the HBT effect for larger values of $-q^2$ than those corresponding to this scale. But it is not known whether there are in addition *larger* size-scales in space-time (i.e. smaller in energy-momentum space) because to see this we would need precise measurements down to very small relative energy-momentum vectors q.

The HBT effect discussed above stems from the squaring of the (symmetrised) amplitude in Eq. (14.3) and the neglect of all contributions which do not fulfil the conditions in Eq. (14.4). Let us assume that the sums in Eq. (14.2) converge to a regular function F:

$$A_{12} \to \int dx_j f(x_j) \exp(-ik_1 x_j) \int dx_l \exp(-ik_2 x_l) f(x_l) \to F(k_1) F(k_2). \tag{14.12}$$

Using the same arguments as before we find that the single rate is then $|F(k)|^2$ and the 'double' rate is $|F(k_1)|^2 |F(k_2)|^2$. This means that in this case we simply obtain the result

$$C_{12}^{coh} = 1 \tag{14.13}$$

without the second, chaotic, term which occurs in Eq. (14.10)! This second limit is called the *totally coherent limit*. The term 'coherent' has been introduced because this is the result if we use the coherent states in a field theory coupled to external sources (this case is considered in Chapter 3). There the probability for emission of one or two quanta with given

https://doi.org/10.1017/9781009401296.014 Published online by Cambridge University Press

energy-momenta depends only upon the square of the Fourier transform of the external current density. This corresponds to the source density discussed above. There are no chaotic phases in this case.

In Chapter 6 we discussed a simple model for particle production, [39]. In that model the final-state particles stem from the application of an external current to the Schwinger model; then this particular coherent state is obtained as a description of the reaction of the quantised dipole density field. This led to early predictions that there should be no HBT effect in a simple particle-production process such as e^+e^- annihilation. The fact that there is and that it can be explained within the Lund model is an explicit proof that there are basic dynamical differences between the Schwinger model with an external source and the Lund model.

There has been intense theoretical discussion of whether the sources in high-energy particle physics are *partially chaotic*, meaning that we might have a scenario which is in between the chaotic HBT and the coherent-state results. We will not develop this discussion here; we refer the interested reader to the reviews [93].

Before we turn to the Lund model interpretation we will comment upon the effects arising when the production regions are in large relative motion, which they evidently are in the Lund model as well as in any other relativistically covariant multiparticle production scenario.

2 *The effect of moving sources on the HBT effect*

The discussion of the HBT effect given above is sufficient for its application in astronomy where there are, very probably, many photon emission sources with (relative) chaotic phases. But they are all at rest or at least moving slowly with respect to each other. This is not the case for high-energy multiparticle production.

In the Lund model we have learned that the particle production structure is that, in the mean, all particles are produced after a certain proper time in the local rest frame. Thus the particle production points are scattered around a hyperbola in space-time $t^2 - x^2 = \tau^2$. The full particle production region has a large longitudinal extension, $L \sim \sqrt{s}/\kappa$, for the production sources, although each vertex is governed by τ.

There is, however, also a strong correlation between the particle production points $x \sim \gamma(v)\tau$ and the momentum $p \sim mv\gamma(v)$, where we use the usual notation for velocity v and the Lorentz contraction factor $\gamma^{-1} = \sqrt{1 - v^2}$. This means that particles from distant parts of the production region will typically exhibit large momentum differences. Consequently the probability of finding particles from opposite ends of a two-jet event with momenta less than $1/L$ (which is necessary to obtain significant interference effects) should be negligible. Therefore the length

https://doi.org/10.1017/9781009401296.014 Published online by Cambridge University Press

scale measured by the HBT effect in this case is not L; *it is instead the distance apart of production points for which the momentum distributions of the produced particles will still overlap.*

In order to get an estimate of the length scale inside which a particular source will deliver its final-state particles let us assume that we have a decay distribution which is completely isotropic in the rest frame of the source. We define the rapidity with respect to some axis. We will neglect the rest masses of the decay products, so that a particle produced along a direction at an angle θ to the rapidity axis will have the rapidity

$$y = \frac{1}{2}\log\left(\frac{E + p_\ell}{E - p_\ell}\right) = \log\cot\frac{\theta}{2} \tag{14.14}$$

where we have used $p_\ell = E\cos\theta$. Expressed in terms of this (pseudo)-rapidity variable we find the isotropic angular distribution

$$\sin\theta\, d\theta d\phi \quad \rightarrow \quad d\phi dy \frac{1}{\cosh^2 y} \tag{14.15}$$

The angle ϕ is the azimuthal angle around the rapidity axis. Thus in this case a typical particle source will produce particles inside a rapidity region with a width around 0.7 rapidity units. We conclude that the particle distributions from sources moving with a rapidity difference Δy will overlap reasonably well as long as $\Delta y \leq 1$.

Therefore this exercise shows that the HBT effect actually must correspond to the measurement of a source size of the order of the local proper time scale, i.e. $\tau \ll L$. In particular the distributions should hardly look more elongated in the longitudinal than in the transverse direction with respect to the main axis and the measured distributions should be independent of the cms energies involved.

3 *The interference effect in the Lund model*

In Fig. 14.1 we exhibit again the breakup of the Lund string into many final-state yoyo-hadrons, which stem from the combination of q- and $\bar{q}$-particles from adjacent vertices. In the same figure we show (by a broken line) the production of the very same final state but in this case the two particles, denoted 1 and 2, have been interchanged.

If these two particles are identical bosons then the amplitudes corresponding to the two possibilies shown in Fig. 14.1 will interfere according to quantum mechanics. We have up to now considered only the probabilities, and not the amplitudes, for the production processes in the Lund model. But, in connection with the discussion in Chapter 11 of the Wilson loop-integral analogy to the production process, we did provide a tentative

https://doi.org/10.1017/9781009401296.014 Published online by Cambridge University Press

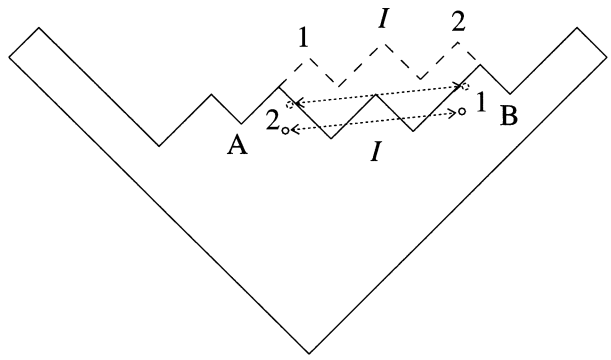

Fig. 14.1. The breakup situation when two identical bosons, 1 and 2, are produced in the Lund model together with an *intermediate* state I and a set of hadrons outside the regions between the points A and B. The distance between the centres of the yoyo-hadrons is shown by the dotted arrows.

matrix element of the following form:

$$\mathcal{M} = \exp(i\xi A), \quad \xi = 1/2\kappa + ib/2 \tag{14.16}$$

The area A is as usual the space-time region (in energy-momentum space units) swept out before the string breaks. Note that throughout we use the lightcone-metric area just as we did in the derivation of the Lund model fragmentation functions. This means that it is a factor of two larger than the 'true' area and we have corrected for this with the factor $1/2$ in the real part of the parameter ξ.

We note in particular that *the areas are not the same in the two cases.*

Thus for the configuration shown by solid lines in Fig. 14.1 we have an area A_{12} in the matrix element $\mathcal{M}_{12}$ and for the one that includes the broken lines we have an area A_{21} in the matrix element $\mathcal{M}_{21}$. The production of the state with two identical bosons 1 and 2 must then be described by the symmetrised matrix element

$$\mathcal{M} = \mathcal{M}_{12} + \mathcal{M}_{21} \tag{14.17}$$

From this we conclude that the probability will contain the factor

$$\begin{aligned} |\mathcal{M}|^2 &= |\mathcal{M}_{12}|^2 + |\mathcal{M}_{21}|^2 + 2\,\mathrm{Re}\,\mathcal{M}_{12}^*\mathcal{M}_{21} \\ &= [\exp(-bA_{12}) + \exp(-bA_{21})]\,(1 + \mathcal{H}) \end{aligned} \tag{14.18}$$

with

$$\mathcal{H} = \frac{\cos(\Delta A/\kappa)}{\cosh(b\Delta A/2)} \tag{14.19}$$

https://doi.org/10.1017/9781009401296.014 Published online by Cambridge University Press

These formulas are proved by straightforward algebra from the area law in Eq. (14.17).

The result is evidently that we may obtain the final state either through the channel '12' or through the channel '21'. *But the interference between the two situations will result in a multiplicative enhancement factor* corresponding to the term $1 + \mathscr{H}$, which depends upon the area difference ΔA between the two space-time breakups. This area difference will depend not only upon the two particles 1 and 2 but also upon the state produced in between, which we have denoted by I in the figure. We note that the area difference exactly vanishes if the energy momentum vectors p_1 and p_2 are equal but grows rapidly from zero with the mass of the state I.

Before we provide formulas for ΔA we note that if two identical *charged* pions are produced then it is necessary to have the state I in between in order to compensate the quantum numbers. Thus if 1, 2 are positively charged pions then it is necessary to compensate by a state of negative charge, and vice versa if they are negatively charged pions. *If two neutral pions are produced, however, then there is no such requirement.* Consequently in an ideal world where it would be just as possible to make measurements on neutral pions as on charged ones we would obtain by straightforward means a smaller area for the neutral pions in general, and the model could thus be easily checked. Up to now this has not been possible because it is very difficult to disentangle a signal from two neutral pions with sufficient precision. They each decay predominantly to a two-photon state, and it is very difficult to pick out four photons with sufficient precision in multiparticle surroundings.

We will provide two different formulas for the area difference ΔA. The first one corresponds to an energy-momentum description:

$$\Delta A = |p_1 E_2 - p_2 E_1 + (p_1 - p_2)E_I - (E_1 - E_2)p_I| \tag{14.20}$$

in easily understood notation. This is the true area, i.e. without the use of the lightcone metric and relevant to the result in Eq. (14.19). We note that it will vanish when the energy-momentum vectors of the bosons are equal and that it will grow quickly with the intermediate-system mass.

Another form that is interesting is obtained by rewriting ΔA as

$$\frac{\Delta A}{\kappa} = |(p_1 - p_2)\delta x - (E_1 - E_2)\delta t| \tag{14.21}$$

and it is easy to construct the space and time differences $\delta x, \delta t$ which will fulfil Eq. (14.21):

$$\begin{aligned} \kappa \delta t &= p_I + \frac{p_1 + p_2}{2} \\ \kappa \delta x &= E_I + \frac{E_1 + E_2}{2} \end{aligned} \tag{14.22}$$

https://doi.org/10.1017/9781009401296.014 Published online by Cambridge University Press

These are the space-time difference vectors between the centres of the two-particle yoyos during the cycle when, according to the Lund model interpretation, they are produced. These points are indicated in the figure and we note that although they do not coincide in the two cases their difference vector is, of course, the same.

With this interpretation of the area difference the result for the correlation term $\mathscr{H}$ in Eq. (14.19) is in a very natural way related to the chaotic correlation $\mathscr{R}$ which we obtained in Eq. (14.11); the phase difference between the two 'production points' occurs weighted by a denominator.

We can also easily understand that this phase difference is, in the Lund string model, related to the fact that there must in general be something else produced in between the pair. This intermediate state, called I above, is needed in order to conserve the quantum numbers in the production process. In this interpretation *the HBT effect measures the region inside which the quantum numbers of the production process are compensated.*

4 *The introduction of transverse momentum*

Before we compare the model to the experimental data it is necessary to account for transverse momentum generation and for the fact that many particles are not directly produced but come from the decay of resonances.

By means of the tunnelling mechanism described by WKB methods in Chapter 11 (cf. also Chapter 12), we should in the Lund model introduce the real factors

$$\exp[-\pi\mu_\perp^2)/(2\kappa)] \tag{14.23}$$

in the matrix element at each production vertex. The quark-mass factors will be the same. But it is necessary to generate different transverse momenta for the two cases at the two vertices adjoining the state I, in order to obtain the same states. In order to see this we note that the transverse momentum $\mathbf{k}_j$ generated at the vertex j can be expressed in terms of the transverse particle momenta $\mathbf{p}_\perp$ as

$$\mathbf{k}_j = \sum \mathbf{p}_\perp \tag{14.24}$$

The sum runs over all particles from one end of the string to the production point of the given q or $\bar{q}$. When the two particles are exchanged and there is a nonvanishing transverse momentum vector difference, $\mathbf{p}_{\perp 1} - \mathbf{p}_{\perp 2} \neq \mathbf{0}$, then this will result in changes in the transverse momentum generated at the q and the $\bar{q}$.

This means that the denominator term in $\mathscr{H}$ from Eq. (14.19) will change as follows:

$$\cosh(b\Delta A/2) \quad \rightarrow \quad \cosh(b\Delta A/2 + \delta_\perp) \tag{14.25}$$

https://doi.org/10.1017/9781009401296.014 Published online by Cambridge University Press

where

$$\delta_{\perp} = \frac{\pi\Delta(\sum \mathbf{k}^2)}{2\kappa}$$

and $\Delta(\sum \mathbf{k}^2))$ means the necessary changes in the sum. Note that the numerator stems entirely from the imaginary phases.

5 *The resonance decay problems*

A much more involved problem is the treatment of the particles which stem from the decay of directly produced resonances. We will briefly discuss what one should expect from a phenomenological treatment of the resonances in terms of Breit-Wigner form factors.

A decaying state with mass m must have in its own rest frame a wave function ψ satisfying

$$\psi \sim \exp(-imt - t\Gamma/2) \text{ so that } |\psi|^2 \sim \exp(-\Gamma t) \tag{14.26}$$

if we are to obtain the well-known exponential decay law with lifetime $1/\Gamma$. This means that such a state behaves as if it has a complex mass $m - i\Gamma/2$, which in the limit $\Gamma \to 0$ corresponds to Feynman's prescription for the propagator, as described in Chapter 3.

Accordingly, one describes the propagation of such a state as a solution of the Klein-Gordon (or any other relativistically covariant) equation with this mass value inserted. We start by assuming that the resonance will be produced at the space-time point $x_R \equiv (t_R, \mathbf{R})$ with a certain production amplitude $f(x_R)$. We further assume, for simplicity, that it will decay to a two-particle state with energy-momentum vectors $(\omega_j, \mathbf{k}_j)$, $j = 1, 2$, at the space-time point $x_1 \equiv (t_1, \mathbf{r}_1)$.

There will be a decay amplitude for this, which we obtain by a coherent sum over all space-time points for the wave functions. For simplicity we assume that the decay products are described by plane wave solutions. The amplitude for the propagation and decay is then

$$\begin{aligned} M &= \int dx \mathscr{M}(x), \\ \mathscr{M}(x) &= f(x_R) g_R(t, \mathbf{r}) \exp[-i(k_1 x_1 + k_2 x_1)] \end{aligned} \tag{14.27}$$

Here $x = x_1 - x_R \equiv (t, \mathbf{r})$ and the (radially symmetric) propagation solution to the Klein-Gordon equation for the resonance is

$$g_R(x) = \frac{1}{r} \exp[i(k_R r - \omega_R t)] \tag{14.28}$$

According to the mass assumption above we have the following relation between the (complex) momentum k_R and the energy ω_R of the decaying

https://doi.org/10.1017/9781009401296.014 Published online by Cambridge University Press

resonance:

$$k_R^2 = \omega_R^2 - (m - i\Gamma/2)^2 \tag{14.29}$$

The t-integral yields energy conservation,

$$\omega_R = \omega_1 + \omega_2 \tag{14.30}$$

and the angular integral over $d\Omega$, in the space differential $d^3r = r^2 dr d\Omega$, will yield for the decay-product plane waves

$$\begin{aligned}\int d\Omega \exp[-i(\mathbf{k}_1 + \mathbf{k}_2)\cdot\mathbf{r}] &= \int d\phi d\theta \sin\theta \exp(-i|\mathbf{k}_1 + \mathbf{k}_2| r\cos\theta) \\ &= \frac{4\pi}{|\mathbf{k}_1 + \mathbf{k}_2| r} \sin(|\mathbf{k}_1 + \mathbf{k}_2| r)\end{aligned} \tag{14.31}$$

Finally the integral over r, now combined with Eq. (14.31), will be proportional to

$$\begin{aligned}&\frac{1}{2|\mathbf{k}_1 + \mathbf{k}_2|}\left(\frac{1}{k_R - |\mathbf{k}_1 + \mathbf{k}_2|} + \frac{1}{k_R + |\mathbf{k}_1 + \mathbf{k}_2|}\right) \\ &\quad = \frac{1}{\omega_R^2 - (m - i\Gamma/2)^2 - (\mathbf{k}_1 + \mathbf{k}_2)^2} \\ &\quad = \frac{1}{M_{12}^2 - (m - i\Gamma/2)^2}\end{aligned} \tag{14.32}$$

This is the well-known Breit-Wigner form factor, which relates the squared mass of the final two-particle state, $M_{12}^2 = (k_1 + k_2)^2$, to the complex mass of the decaying resonance. We have used the relations in Eqs. (14.29) and (14.30) in the last two lines and have left out a set of constant factors along the way, together with the remaining production amplitude factor $f(x_R)\exp[-i(k_1 + k_2)x_R]$.

There is evidently a close relationship between the Breit-Wigner distribution and the Feynman propagator in energy-momentum space. This means that the distribution in mass for the final-state particles will be proportional to $|M|^2$ and thus to

$$\frac{1}{(M_{12}^2 - m^2 + \Gamma^2/4)^2 + m^2\Gamma^2} \tag{14.33}$$

When we consider the correlation between a pion stemming from this kind of decay and one stemming from direct production it is necessary to symmetrise the wave functions etc. Bowler, [35], has done this for us and for the details we refer to his treatment of both this and a number of other final-state corrections to the HBT effect.

The result of such considerations is that if we have a 'spectator state' from the resonance decay, which with Bowler's notation we will call 3,

https://doi.org/10.1017/9781009401296.014 Published online by Cambridge University Press

together with two interfering bosons 1 and 2 then if the width of the resonance Γ in the formula above fulfils

$$\Gamma < |M_{13} - M_{23}| \tag{14.34}$$

the interference effects will vanish. There is consequently no HBT enhancement effect for the decay products from sufficiently long-lived resonances. The question is then what we mean by 'long-lived'. To ascertain this, we investigated three different situations in [22], where the original Lund interpretation occurs.

1 Only charged or neutral pions are produced within the Lund model scenario. This is evidently not in accordance with the experimental observations for e^+e^- annihilation reactions but it does actually provide a reasonably good description of many features of the final states.

2 There is the usual mixture in the Lund model of stable and unstable particles, including strange particles and baryons. The matrix elements are in each case evaluated for the stable final particles, ignoring the fact that some of them come from resonances.

3 The decay products of a resonance with four-vector energy-momentum k, mass m and width Γ are allowed to contribute to the HBT effect only if $kq \leq m\Gamma$. Here q is the the four-momentum difference vector.

In [22] we compared the data from the TPC collaboration at SLAC-PEP to three different cases obtained by a Monte Carlo simulation of the Lund model predictions, with a weighting of each event by the factor $1 + \mathscr{H}$ in Eq. (14.19). It was found, firstly, that cases 1 and 2 above coincided with each other from all practical points of view and also with the data. It turns out that the results are essentially only sensitive to the numerator in $\mathscr{H}$, i.e. there is a quick falloff in the cosine function for $\kappa \simeq 0.2-0.3$ GeV^2, which we have been using in the Lund model. The hyperbolic cosine in the denominator only takes over after the cosine function has gone down to zero. The reason for this is that the b-parameter in the Lund model is essentially smaller than the scale provided by κ.

Case 3 is, however, very far from the data and the predicted HBT effect is very small. There are, according to the Particle Data Group tables, a set of long-lived resonances which may affect the results. Bowler, [34], has shown that the major problem is actually the rate of produced η'-mesons in the Lund model. Remember that in Chapter 12 we have already presented some problems related to the rate of the η'-particles in the Lund model.

https://doi.org/10.1017/9781009401296.014 Published online by Cambridge University Press

Bowler found that around 40% of the like-sign pion pairs which come out with Q-values ($Q^2 = -q^2$) below 0.2 GeV stem from η'-decays. Further, the pions from other decays of long-lived resonances do not in general populate this region at all. This means that at the q-value range, where it matters, the long-lived η'-decay products really play a very large role. Bowler then questions the Lund rate of η'-production and as we mentioned in Chapter 12 the model predictions may well be wrong. Bowler finds that if there were a strong suppression of η'-particles in the production process and if instead the observed pions were directly produced then almost the same HBT effect as for the cases 1, 2 above is also predicted in case 3.

14.3 The polarisation effects in the Lund model

1 The dynamical idea

We will start with a semi-classical explanation for the existence of a large polarisation effect in the Lund model. We consider the production of a $q\bar{q}$-pair at a vertex and assume that the particles each have mass m and are tunnelling out with compensating transverse momenta $\pm\mathbf{k}_t$.

In order to conserve the energy they will appear on the mass shell at the relative distance $2l = 2m_t/\kappa$, where $m_t = \sqrt{m^2 + \mathbf{k}_t^2}$, as we have discussed several times before. In this way both the energy and the momentum are conserved. *But the angular momentum is not conserved.*

From Fig. 14.2 we immediately conclude that the orbital angular momentum of the pair state is equal to

$$L = 2k_t l = \frac{2k_t m_t}{\kappa} \tag{14.35}$$

in the direction along a unit vector determined by the vector product $\boldsymbol{l} \times \mathbf{k}_t$; the direction of the force field, $\boldsymbol{l}$, is then defined to go from the produced $\bar{q}$ to the q, q having the transverse momentum $\mathbf{k}_t$.

The size of L can by the usual tunnelling formulas be estimated from Eq. (14.35) to be very close to unity for an average transverse momentum size. Therefore the effect cannot be small for this average situation. It is also reasonable to assume that the force field, unless there are local excitations, should contain no angular momentum. So, the only way in which this increase in the orbital angular momentum can be compensated is if the combined spin of the produced pair S equals 1 (they are spin 1/2 particles) and if the transverse component of $\mathbf{S}$ is oppositely directed to the vector $\mathbf{L}$.

This means in spectroscopical notation that such pairs are produced in a state with the assignment $^3P_0$, meaning that a triplet spin state $S = 1$ combines with an orbital angular momentum state $L = 1$ to give

https://doi.org/10.1017/9781009401296.014 Published online by Cambridge University Press

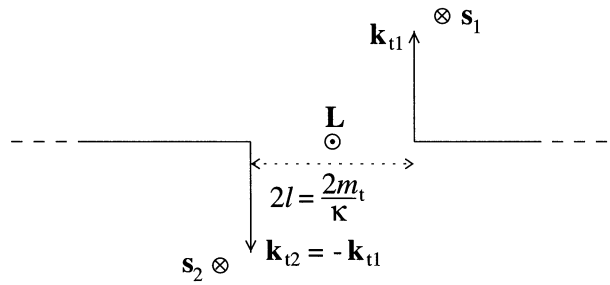

Fig. 14.2. A $q\bar{q}$-pair is produced with oppositely directed transverse momenta at a typical distance for a force field with finite energy density κ. The vector $\mathbf{L}$ points transversely outwards while the compensating spin vectors $\mathbf{s}_1, \mathbf{s}_2$ point inwards.

a state with total angular momentum $J = 0$. It turns out that owing to the intrinsic parity of the $q\bar{q}$-pair (which results in pseudoscalar spin 0 mesons) this state exactly corresponds to the quantum numbers of the vacuum ($L = 1$ states have negative parity).

The model also contains, however, predictions for the relative spin direction from a knowledge of the force field direction and the transverse momentum of the q or $\bar{q}$ with respect to the field. We will later show the consequences in connection with Λ-polarisation in a baryon fragmentation region.

2 *The corresponding situation in QED*

It is of some interest to note that there will be a very different result for the production of an e^+e^--pair in an external electric field.

To see this we assume that we have exactly the same production situation in QED as the one described above; let us also for the sake of argument assume that the pair will be polarised in the same way as above. Then *in QED this polarisation will not be conserved.*

The reason is that when the charges separate in the external field with momenta transverse to the field direction, see Fig. 14.3, then each of the charged particles will be accelerated along the electric field. But they will also cross the electric field lines, which means basically that there will be a torque working on the spin of the particles. Therefore the field will quickly take back the possible spin and kill the polarisation effects.

In order to discuss this effect in detail we consider the equation of motion for a spin vector in the particle's rest frame. In this frame the field, which was a constant electric field in the frame where the particle

https://doi.org/10.1017/9781009401296.014 Published online by Cambridge University Press

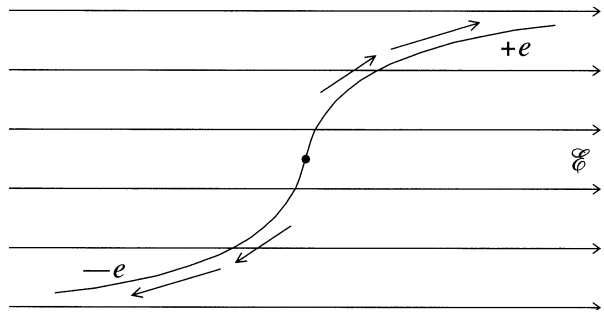

Fig. 14.3. The motions of an oppositely charged $\pm e$ pair in an external field $\mathscr{E}$.

was produced, is not purely electric. (The following discussion partly uses arguments from Jackson's book.)

The effect was noticeable for the fields we exhibited in a moving frame in connection with the method of virtual quanta in Chapter 2. There we found that a magnetic field was induced:

$$\mathscr{B} = -\mathbf{v} \times \mathscr{E} \tag{14.36}$$

and this is true in general ignoring correction terms of order v^2. Here also in the rest frame of the electron there is an induced magnetic field of this size.

A particle with spin $\mathbf{s}$ also has a magnetic moment $\boldsymbol{\mu}$ proportional to the spin vector:

$$\boldsymbol{\mu} = \frac{ge}{2m}\mathbf{s} \tag{14.37}$$

with the g-factor (as normal for a Dirac particle) equal to 2. (We will in the next section find the Thomas-precession correction to this result.)

Therefore there is an equation of motion for the spin

$$\frac{d\mathbf{s}}{dt} = -\boldsymbol{\mu} \times \mathscr{B} \tag{14.38}$$

which corresponds to an extra term in the hamiltonian

$$H' = -\boldsymbol{\mu} \cdot \mathscr{B} = \boldsymbol{\mu} \cdot (\mathbf{v} \times \mathscr{E}) \tag{14.39}$$

This means that in order to minimise the energy, the magnetic moment and therefore also the spin should be directed oppositely to $\mathbf{v} \times \mathscr{E}$.

This is exactly the opposite result to that obtained from the simple model described above. There we required that the spin should be oppositely directed to the 'produced' orbital angular momentum, which is directed along the direction $\mathbf{l} \times \mathbf{k} \propto \mathscr{E} \times \mathbf{v}$.

https://doi.org/10.1017/9781009401296.014 Published online by Cambridge University Press

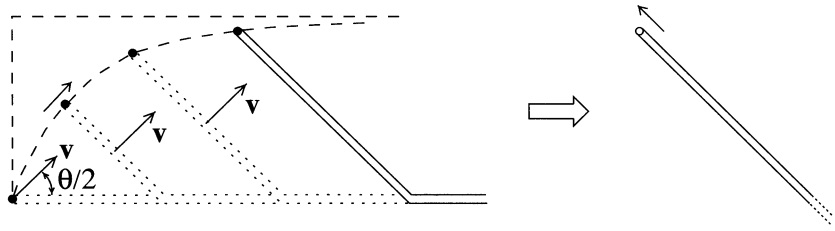

Fig. 14.4. The motion of a particle attached to a string (*a*) before and (*b*) after a boost to the rest system of the string piece adjoining the endpoint.

In the Lund model, however, there will be no such effect in a confined string situation. If we go back to the (admittedly classical) picture of the transverse motion of a particle attached to a string in Chapter 12 then we may utilise a frame in which the adjoining string piece is at rest, see Fig. 14.4.

This means that we are boosting in the transverse direction of the string piece, along the angle $\pi/4$ in Fig. 14.4(*a*), with velocity $v = \cos(\pi/4) = 1/\sqrt{2}$. In this frame we will find that the endpoint particle is simply moving outwards along a straight string, i.e. *there is always only a color electric field* acting on the particle. Therefore in a confined scenario of the Lund model type we do not have the torque on the spin discussed above.

This is actually the reason why we did not present calculations of how spin 1/2 particles would tunnel out of a confining force field. For particles with spin it is not sufficient to choose a potential that describes a purely electrostatic external field if we want to account for the relation between the force field and the particle in a confining situation. It is necessary to define a more general potential in such a way that *in the rest frame of the particle* the field is electrostatic.

3 *The Thomas-precession effect and a different model*

The result in Eq. (14.39) is actually identical to the so-called spin-orbit coupling in spectroscopy. For that case we write the following formula for the electric field in an atom as

$$e\mathscr{E} = -\frac{\mathbf{r}}{r}\frac{dV}{dr} \tag{14.40}$$

in terms of a spherically symmetric potential $V(r)$. This means that the

https://doi.org/10.1017/9781009401296.014 Published online by Cambridge University Press

spin-dependent term in the hamiltonian is

$$\frac{g}{2m^2}\mathbf{s}\cdot(\mathbf{r}\times m\mathbf{v})\frac{1}{r}\frac{dV}{dr} = \frac{g}{2m^2}\mathbf{s}\cdot\mathbf{L}\left(\frac{1}{r}\frac{dV}{dr}\right) \tag{14.41}$$

The only problem is that the g-factor according to all experimental observations should equal 1 and not 2 as suggested by Uhlenbeck and Goudsmit. The puzzle was solved by Thomas, who pointed out that there is a subtle relativistic effect when a spinning particle is accelerated. The effect comes very nicely out of the relativistically covariant description of a spinning particle in the Dirac equation.

We will not derive the Thomas effect in detail because we would then need an extensive formalism for $(3+1)$-dimensional Lorentz transformations. It is done in Jackson's book and we refer readers interested in the details to this. It is, however, a purely kinematical effect. The spinning particle may, in its own rest frame, have any spin vector direction. For the observer who is accelerated with respect to this rest frame there will be a bias in the direction of the coordinate system in the rest frame relative to that in the observer's frame.

Suppose that the observer adjusts his coordinate axes to coincide with those in the particle's rest frame at a time, t, when the particle has a certain velocity $\mathbf{v}(t)$. Then after a moment dt the particle will have the velocity $\mathbf{v}(t+dt) = \mathbf{v}(t) + d\mathbf{v}$.

Therefore when the observer compares the axes after the time increment dt he will have to make a Lorentz boost along the new direction. As we have said in Chapter 2, Lorentz boosts in different directions do not commute. In other words $L(\mathbf{v})L(d\mathbf{v}) \neq L(\mathbf{v}+d\mathbf{v})$, where L is the boost operator, unless $\mathbf{v}$ and $d\mathbf{v}$ are parallel.

Consequently, the coordinate axis, and also the spin direction in the rest frame, will seem for the external observer to be rotating at a rate given by the Thomas angular velocity:

$$\boldsymbol{\Omega}_T = \frac{\gamma^2}{1+\gamma}\frac{d\mathbf{v}}{dt}\times\mathbf{v} \tag{14.42}$$

In the nonrelativistic approximation $\gamma = 1$, which is relevant for an electron in an atom (an atomic electron moves with an average velocity equal to $\alpha \simeq 1/137 \ll 1$) the acceleration will be given by the force in Eq. (14.40) and therefore the angular velocity will be

$$\boldsymbol{\Omega}_T = \frac{-1}{2m^2}\mathbf{L}\left(\frac{1}{r}\frac{dV}{dr}\right) \tag{14.43}$$

which will give an effective hamiltonian term equal to

$$H_T = \boldsymbol{\Omega}_T\cdot\mathbf{s} = \frac{-1}{2m^2}\mathbf{s}\cdot\mathbf{L}\left(\frac{1}{r}\frac{dV}{dr}\right) \tag{14.44}$$

https://doi.org/10.1017/9781009401296.014 Published online by Cambridge University Press

This is of the same type as the spin-orbit coupling and together they will change the effective g-factor to $g - 1$, i.e. to the observed value.

In this way it is possible to obtain a spin effect that stems from the acceleration of the particle in a direction not parallel to its momentum vector $\mathbf{k}$. Thus if we imagine that after it has been produced the particle is accelerated along the force field direction $\boldsymbol{l}$ then there should be a Thomas precession effect with an effective hamiltonian

$$H'_T = h\mathbf{s} \cdot (\boldsymbol{l} \times \mathbf{k}) \tag{14.45}$$

Here h is a positive-definite coupling constant equal to the force.

Now we do have a favorable situation for the particle to choose its spin in the direction opposite to the vector $\boldsymbol{l} \times \mathbf{k} = \boldsymbol{l} \times \mathbf{k}_t$, which is exactly in accordance with the prediction of the simple Lund polarisation model. In this case it would be the final-state interaction, i.e. the acceleration of the particle into the the final hadronic state, which would produce the polarisation effect, rather than the pair production mechanism, as in the Lund model explanation.

It may seem like magic, because there is really no force on the spin itself. It is instead an observational bias that produces the effect. It has nevertheless been suggested as a possible model to explain polarisation effects in hadronic production processes, [50].

4 *The observable consequences*

It is possible to make a large number of predictions from the simple model we discussed in subsection 1. We will be content, however, to discuss the results for Λ-particle polarisation in a baryon fragmentation region. The Λ-particle is, in some sense, one of the very few unqualified gifts which Nature has bestowed upon high-energy physicists, at least those interested in polarisation physics. Almost every other tool for observation contains very many complications. The reasons why the Λ is so nice are two-fold.

Firstly the Λ-particle decays via weak interactions to a nucleon and a pion. Weak interactions do not conserve parity. Consequently the Λ, through its decay, exhibits an asymmetry in the distribution of the angle between the nucleon and the pion which is directly related to its spin direction. And this asymmetry is large!

Secondly, the structure of a Λ-particle is rather simple. It can be described essentially as a state composed of a diquark $(ud)_0$, the index 0 denoting that the pair has spin and isospin equal to 0, and an s-quark. From this structure we conclude that it is the spin of the s-quark which determines the spin of the Λ-particle.

Thus the observation of Λ-polarisation reveals the direction of the s-quark's polarisation. If a Λ-particle is observed with a large fractional

https://doi.org/10.1017/9781009401296.014 Published online by Cambridge University Press

energy-momentum in the fragmentation region of a proton then it is most probably composed of a $(ud)_0$ diquark stemming from the original proton and a produced s-quark. If we imagine that the s-quark has been produced according to the Lund model prescription backwards along a string adjoining the $(ud)_0$ diquark (cf. the discussion of baryon fragmentation in Chapter 20) then the model of subsection 1 can be applied. It is only necessary to relate the transverse momentum of the produced s-quark to the transverse momentum of the observed Λ.

In the original paper, [9], we made two assumptions. The first was that the polarisation $\mathscr{P}$ of the produced s-quark will increase with the orbital angular momentum L of the $s\bar{s}$-pair and we chose the simple relation

$$\mathscr{P} = \frac{L}{L+\beta} \tag{14.46}$$

with the parameter $\beta \sim 1$–2. We further assumed that both the original diquark $(ud)_0$ and the produced s-quark had gaussian distributions of their transverse momenta, with widths σ_{qq} and σ_q, respectively. For the s-quark this can be justified from the tunnelling mechanism and for the diquark from the Fermi motion in the original baryon state.

This assumption means that the correlation between the momentum of the final-state Λ-particle, $\mathbf{p}_t$, and that of the s-quark, $\mathbf{k}_t$, will be

$$\left\langle \mathbf{k}_t \cdot \frac{\mathbf{p}_t}{|\mathbf{p}_t|} \right\rangle = \frac{\sigma_q^2}{\sigma_q^2 + \sigma_{qq}^2} |\mathbf{p}_t| \tag{14.47}$$

The resulting polarisation for the Λ-particle then agrees very well with the results of the ISR-data, see [9] and [58].

There must be corrections to the results for smaller values of the fragmentation variable z, i.e. the fraction of the original baryon energy-momentum carried by the Λ-particle. There are a set of possible channels that produce a Λ-particle in a baryon fragmentation region, according to the Lund model, cf. Chapter 20. It is then possible to predict the behaviour of the polarisation also for smaller values of the ratio z (or the Feynman variable x_F) in the fragmentation region of the proton and also to use the same mechanism for other hyperons, i.e. strange baryons.

The resulting predictions have been repeatedly confirmed. It is interesting that the polarisation effects are also found in states of a diffractive nature, [106]. Whether the dynamical mechanism for producing polarisation is the one proposed in the Lund model, i.e. the produced states come out with polarisation, or whether it is an effect of final-state Thomas precession is a question that we must leave open until more data on resonance hyperon polarisation become available.